INTERNATIONAL JOURNAL FOR NUMERICAL METHODS IN FLUIDS, VOL. 4, 813–832 (1984)

DIFFRACTION OF WAVES BY SEMI-INFINITE BREAKWATER USING FINITE AND INFINITE ELEMENTS

P. BETTESS*, S. C. LIANG† AND J. A. BETTESS‡

Department of Civil Engineering, University College of Swansea, Singleton Park, Swansea, SA2 8PP

SUMMARY

A finite and infinite element model is derived to predict wave patterns around a semi-infinite breakwater in water of constant depth. Both circular and square meshes of elements are used. The wave theory used is that of Berkhoff. The appropriate boundary conditions for finite and infinite boundaries are described. The singularity in the velocity at the breakwater tip is modelled effectively using the technique of Henshell and Shaw originally developed in elasticity. The results agree well with the analytical solution. In addition the problem of waves incident upon a semi-infinite breakwater and parabolic shoal, where both diffraction and refraction are present, is solved. There is no analytical solution for this case. The combination of finite and infinite elements is found to be an effective and accurate technique for such problems.

KEY WORDS Waves Diffraction Refraction Finite Elements Infinite Elements Breakwater

INTRODUCTION

The theory of wave diffraction has received much attention since the work of Sommerfeld[1] on the diffraction of plane monochromatic light waves by a half plane. Penney and Price[2] showed that the Sommerfeld solution of the diffraction of light is also a solution of the water wave diffraction phenomenon. Wiegel[3] used the exact solution of Penney and Price to calculate and plot the diffraction coefficients for a semi-infinite breakwater. Shou-Shan Fan[4] wrote a computer program to simulate this analytical solution.

In this paper we are concerned with the application of finite element techniques to predict wave patterns around a vertical thin impervious rigid semi-infinite breakwater with constant or varying depth of water in the horizontal plane. The aim is first to reproduce the analytical results and then to generate results for problems for which no analytical solutions are available.

The theory uses a potential representation of the velocities in the fluid with a linearized surface boundary condition. The resulting two dimensional equations must be solved in a domain which is assumed infinite. In general waves come from infinity, and after reflection are radiated to infinity. The radiation of the waves to infinity represents a constant energy loss and the mathematical model of the system must be able to deal with this. The present approach is to model the entire domain using elements, some of which extend to infinity.

* Lecturer
† Research Assistant
‡ Computer Manager

0271–2091/84/090813–20$02.00

Received 8 March 1983
Revised 1 August 1983

An analytical solution computer program written in Algol 68-R and based upon that of Shou-Shan Fan has been developed which predicts the wave height variations around the semi-infinite breakwater. This has been run in the same cases as the present finite element model. The results will be compared later.

THEORY

Berkhoff[5,6] developed an approximate general theory of waves, and the theory presented here is based on his work. The wave equation

$$\nabla . (cc_g \nabla \phi_0) + \frac{\omega^2 c_g}{c} \phi_0 = 0 \tag{1}$$

is obtained, providing terms $O(\nu^2)$ are neglected. In the above equation c, the wave celerity, is given by ω/k where k is wave number and c_g, the group velocity, is given by $c_g = nc$ and

$$n = \tfrac{1}{2}(1 + 2kh/\sinh 2kh) \tag{2}$$

For shallow water waves kh is small and so $\tanh kh = kh$. ν is a parameter[6] $[H/(\lambda L)^{1/2}]$, where λ = mean wave length, L = horizontal length and H = wave height. This leads to $c = (gh)^{1/2}$, and $n = 1$, so that equation (1) becomes the familiar shallow water wave equation

$$\nabla . (h \nabla \phi_0) + \frac{\omega^2}{g} \phi_0 = 0 \tag{3}$$

For deep water kh is large and so $\tanh kh = 1$. This leads to $c = g/\omega$, and $n = 1/2$, so that

$$\nabla^2 \phi_0 + \frac{\omega^4}{g^2} \phi_0 = 0 \tag{4}$$

It is evident that for intermediate but constant depths, equation (1) is correct.

The boundary conditions which the differential equation (1) must satisfy must be specified. On solid boundaries the velocity must be zero and hence $\partial\phi/\partial n = 0$, where n is the outward normal to the surface. This implies total reflection of the wave, such as may occur on an impermeable vertical wall. In real problems the reflection will be partial as energy absorption will occur on a shoaling beach due to wave breaking, or on a real breakwater where the porous nature of the boundary does not result in a zero boundary velocity. For such a boundary, the condition can be written

$$\frac{\partial \bar{\phi}}{\partial n} = \frac{\alpha}{c} \frac{\partial \bar{\phi}}{\partial t} \tag{5}$$

where α is a real dimensionless damping coefficient. $\bar{\phi}$ is the velocity potential which depends upon time, t, and ϕ is the velocity potential for periodic waves, so that $\bar{\phi}(x, y, z, t) = \phi(x, y, z) \exp(i\omega t)$. In terms of complex response the boundary condition becomes

$$\frac{\partial \phi}{\partial n} = \frac{i\omega\alpha}{c} \phi \tag{6}$$

Total reflection is given by $\alpha = 0$, and total absorption by $\alpha = 1$, so it is readily seen that for any partial reflection $0 \leq \alpha \leq 1$. Where the energy absorption is due largely to inertia terms, such as occur in wave breaking, α could be given a complex value. However in view of the

scarcity of experimental data, the determination of such constants is too complicated to be attempted. Austin and Bettess discuss the longshore boundary condition.[7]

The boundary condition which must be imposed as the position of the boundary tends mathematically to infinity is more difficult. Here it is not sufficient to simply require that the ϕ corresponding to outgoing waves tends to zero as the distance tends to infinity, but an additional condition needed is one requiring no return of reflected waves from infinity. If at a large distance from the surface of the disturbance plane waves proceeding in a radial direction are assumed, a general wave form can be written as

$$\bar{\phi} = F_1(r-ct)+F_2(r+ct) \tag{7}$$

where c is the wave velocity. The returning wave, F_2, is now required to vanish. It can be seen that

$$\frac{\partial\bar{\phi}}{\partial r} = F_1' \quad \text{and} \quad \frac{\partial\bar{\phi}}{\partial t} = -cF_1' \tag{8}$$

so this condition can be written as

$$\frac{\partial\bar{\phi}}{\partial r} = -\frac{1}{c}\frac{\partial\bar{\phi}}{\partial t} \tag{9}$$

For periodic motion this condition becomes

$$\frac{\partial\phi}{\partial r} = -\frac{i\omega}{c}\phi \tag{10}$$

The above condition was derived by Zienkiewicz and Newton,[8] and is a special case of the Sommerfeld radiation condition[9,10] which in two dimensions is

$$\lim_{r\to\infty} r^{1/2}\left(\frac{\partial\phi}{\partial r}+\frac{i\omega}{c}\phi\right) = 0 \tag{11}$$

It is essential thus that any formulation of an unbounded wave problem should satisfy this condition either at a finite boundary which is deemed to represent infinite conditions or at infinity itself, if it is included in the mathematical model. Although equation (10) only applies, strictly, to plane waves, normally incident upon the boundary, as the radius at which the boundary is placed is increased it will tend towards the exact boundary condition. The above conditions apply only to the reflected wave, not the incident wave.

VARIATIONAL FORMULATION AND DISCRETIZATION

General statement

The numerical solution of equation (1) will now be discussed, for which purpose it will be convenient to split the domain of the problem into inner and outer parts. The velocity potential in the outer domain is written

$$\phi = \phi^{\mathrm{I}}+\phi^{\mathrm{R}} \tag{12}$$

Where ϕ^{I} is the known incident wave and ϕ^{R} is the outgoing wave, unknown at present. The variational functional from which equation (1) arises can now be written as

$$\pi = \iint \frac{1}{2}\left[cc_{\mathrm{g}}(\nabla\phi)^2-\frac{\omega^2 c_{\mathrm{g}}}{c}\phi^2\right]\mathrm{d}x\,\mathrm{d}y-\int_{s_1}\tfrac{1}{2}i\omega\alpha c_{\mathrm{g}}\phi^2\,\mathrm{d}s \tag{13}$$

The natural boundary condition now corresponds to equation (6) on the boundary S_1. In the outer domain the same functional is used but now equation (12) is substituted, i.e.

$$\pi = \iint \frac{1}{2}\left[cc_g(\nabla(\phi^I+\phi^R))^2 - \frac{\omega^2 c_g}{c}(\phi^I+\phi^R)^2\right] dx\, dy \tag{14}$$

The Euler–Lagrange equation obtained by varying ϕ^R is equation (1), and the natural boundary condition (6), is also obtained (see, for example, Reference 11).

The outer domain functional can be simplified. The quadratic terms in ϕ^I are not subject to variation and can thus be discarded. As ϕ^I is already a solution of continuity equation, the linear terms in ϕ^I can be transformed to a line integral on the inner domain boundary. This is done as follows.

$$\iint \frac{1}{2}\left[cc_g\{\nabla(\phi^I+\phi^R)\}^2 - \frac{\omega^2 c_g}{c}(\phi^I+\phi^R)^2\right] dx\, dy = \iint \frac{1}{2}\left[cc_g(\nabla\phi^R)^2 - \frac{\omega^2 c_g}{c}\phi^{R^2}\right] dx\, dy$$
$$+ \iint \left[cc_g\left\{\left(\frac{\partial\phi^I}{\partial x}\frac{\partial\phi^R}{\partial x}\right)+\left(\frac{\partial\phi^I}{\partial y}\frac{\partial\phi^R}{\partial y}\right)\right\} - \frac{\omega^2 c_g}{c}\phi^I\phi^R\right] dx\, dy \tag{15}$$

Consider the second term of the right hand side of equation (15).

$$\iint \left[cc_g\left\{\frac{\partial}{\partial x}\left(\frac{\partial\phi^I}{\partial x}\phi^R\right)+\frac{\partial}{\partial y}\left(\frac{\partial\phi^I}{\partial y}\phi^R\right)\right\}\right] dx\, dy$$
$$- \iint \left[cc_g\left(\frac{\partial^2\phi^I}{\partial x^2}\phi^R + \frac{\partial^2\phi^I}{\partial y^2}\phi^R\right) + \frac{\omega^2 c_g}{c}\phi^I\phi^R\right] dx\, dy \tag{16}$$

The last term of equation (16) can be written as

$$\iint \left[cc_g\left(\frac{\partial^2\phi^I}{\partial x^2}+\frac{\partial^2\phi^I}{\partial y^2}\right)+\frac{\omega^2 c_g}{c}\phi^I\right]\phi^R\, dx\, dy \tag{17}$$

For constant depth, implying constant c and c_g, the term in square brackets above is automatically zero, because ϕ^I, by definition, satisfied equation (1). Using Green's theorem and the preceding arguments, the functional for the waves in the outer region can be written as

$$\pi = \iint \frac{1}{2}\left[cc_g(\nabla\phi^R)^2 - \frac{\omega^2 c_g}{c}\phi^{R^2}\right] dx\, dy + \oint cc_g\left[\frac{\partial\phi^I}{\partial x}\phi^R\, dy - \frac{\partial\phi^I}{\partial y}\phi^R\, dx\right] \tag{18}$$

The second term of equation (18) vanishes at the infinitely distant boundary as ϕ^R and $\partial\phi^R/\partial n$ both become zero there in addition to the requirement of equation (11). On the inner boundary integral produces a 'forcing' term.

The only restriction on the incoming wave in this formulation is that it is a solution of the wave equation. As analytical wave equation solutions are relatively rare, the computer program described later allows only two kinds of incident waves. These are a plane monochromatic wave, and the same wave plus its total reflection at an infinite straight wall.

Finite and infinite elements

To discretize the problem in the standard finite element manner it is necessary to describe the unknown function ϕ or ϕ^R in terms of nodal parameters, a_i, and prescribed shape functions, as for example

$$\phi = N_i a_i \tag{19}$$

Minimizing with respect to nodal parameters results in the usual finite element forms, which are described in standard texts.[12] Two finite elements are used in the inner region. These are isoparametric forms of the 6 noded triangle and the 8 noded quadrilateral elements. Detailed formulations are given in Reference 12, and standard numerical integration procedures using Gauss–Legendre numerical integration[13] are followed.

In the outer domain, which extends to infinity, a different approach is necessary. Here either a boundary integral form of solution can be attempted, or special infinite elements[14] can be developed, which approximate to the true solution. Here the second approach will be adopted.

Infinite element—numerical integration

The radial direction within the infinite element is denoted by the co-ordinate s, which must have the same metric as the x, y co-ordinates of the problem, unlike ξ.[15]

At each integration point within the element the derivatives needed in the functional can be found by transforming them from s, η co-ordinates to x, y co-ordinates, using the Jacobian matrix based on the original finite shape function, and the integration can proceed numerically as usual.[12]

In the s direction of course Gauss–Legendre numerical integration is not appropriate. Gauss–Laguerre numerical integration was originally used instead.[13,14] This is often used for potential infinite elements and it proved moderately successful here. However large numbers of sampling points were needed in the s direction to achieve reasonable accuracy. (Up to 32 points were used). This was due to the approximation by the integration formula of a harmonic function e^{iks} as a polynomial.

It seemed that a specially designed integration formula might be more effective. An integration formula essentially similar to the Newton–Cotes formulae was devised, to account for the harmonic terms in the shape function. The formula evaluates integrals of the form

$$\int_0^\infty P(s)e^{-\alpha s}e^{i\beta s}\,ds \tag{20}$$

where $P(s)$ is a polynomial and α and β are constants. The sampling points were chosen arbitrarily to be at $(2n+1)/4$ multiples of the wavelength. This seemed reasonable as it avoided the zeros of the real and imaginary parts of $e^{i\beta s}$. A series of formulae for polynomials up to quintic was developed and checked. As an example the three point formula is here derived. The polynomial $P(s)$ is expressed in terms of Lagrange polynomials, and the values of P at the first 3 integration points ($s = \pi/4\beta$, $3\pi/4\beta$ and $5\pi/4\beta$) so that

$$P = L_1P_1 + L_2P_2 + L_3P_3 \tag{21}$$

Where L_i are the Lagrange polynomials. Equation (21) is integrated, to give

$$\int_0^\infty Pe^{-\alpha s}e^{i\beta s}\,ds = P_1\int_0^\infty L_1e^{-\alpha s}e^{i\beta s}\,ds + P_2\int_0^\infty L_2e^{-\alpha s}e^{i\beta s}\,ds + P_3\int_0^\infty L_3e^{-\alpha s}e^{i\beta s}\,ds \tag{22}$$

The three integrals give the weights in the integration formula. The first weight will be evaluated here.

$$L_1 = \left(\frac{3\pi}{4\beta} - s\right)\left(\frac{5\pi}{4\beta} - s\right)\Big/\left(\frac{3\pi}{4\beta} - \frac{\pi}{4\beta}\right)\left(\frac{5\pi}{4\beta} - \frac{\pi}{4\beta}\right) \tag{23}$$

$$L_1 = \frac{15}{8} - \frac{4\beta}{\pi}s + \frac{2\beta^2}{\pi^2}s^2 \tag{24}$$

Table I. Abscissas and weights for integrals of the form

$$\int_0^\infty P(s)e^{-\alpha s}e^{i\beta s}\,ds$$

Abscissa	Weight $\left(r=\dfrac{\alpha+i\beta}{\alpha^2+\beta^2}\right)$
$\dfrac{\pi}{4\beta}$	$\dfrac{15}{8}r-\dfrac{4\beta}{\pi}r^2+\dfrac{4\beta^2}{\pi^2}r^3$
$\dfrac{3\pi}{4\beta}$	$-\dfrac{5}{4}r+\dfrac{6\beta}{\pi}r^2-\dfrac{8\beta^2}{\pi^2}r^3$
$\dfrac{5\pi}{4\beta}$	$\dfrac{3}{8}r-\dfrac{2\beta}{\pi}r^2+\dfrac{4\beta^2}{\pi^2}r^3$

The equality

$$\int_0^\infty s^n e^{(-\alpha+i\beta)s}\,ds=\left(\frac{\alpha+i\beta}{\alpha^2+\beta^2}\right)^n(n-1)! \tag{25}$$

is now used to give

$$\int_0^\infty L_1 e^{-\alpha s}e^{i\beta s}\,ds=\frac{15}{8}\left(\frac{\alpha+i\beta}{\alpha^2+\beta^2}\right)-\frac{4\beta}{\pi}\left(\frac{\alpha+i\beta}{\alpha^2+\beta^2}\right)^2+\frac{4\beta^2}{\pi^2}\left(\frac{\alpha+i\beta}{\alpha^2+\beta^2}\right)^3 \tag{26}$$

The other weights can be found similarly, and the extension to formulae with more weights is straightforward. The three point formula shown in Table I evaluates exactly the element matrix for the parent element shape and this was checked analytically.

In practice a 6 point formula has been used most often and an economy over the Gauss-Laguerre integration is achieved.

ANALYTICAL SOLUTION

The problem of diffraction around a semi-infinite breakwater has been solved by Sommerfeld[1] and Penney and Price,[2] and a numerical evaluation of the solution can be found in Reference 4. The incident wave makes an angle of θ_0 degrees with the positive x-axis (see Figure 1). The solution at a point P with cylindrical co-ordinates (r, θ, z) is by

$$\phi = A\exp(i\omega t)\cosh[k(z+h)]F(r,\theta) \tag{27}$$

and the free surface can be given by

$$\eta=\frac{Ai\omega}{g}\cosh(kh)\exp(i\omega t)F(r,\theta) \tag{28}$$

with

$$F(r,\theta)=f(\sigma)e^{-ikr\cos(\theta-\theta_0)}+f(\sigma')e^{-ikr\cos(\theta+\theta_0)} \tag{29}$$

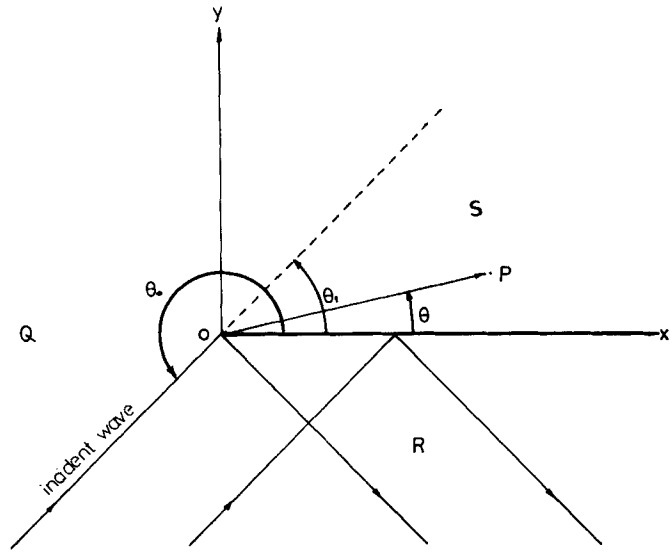

Figure 1. Geometry of semi-infinite breakwater diffraction problem

where

$$\sigma = 2\left(\frac{kr}{\pi}\right)^{1/2} \sin \tfrac{1}{2}(\theta - \theta_0) \tag{30}$$

$$\sigma' = -2\left(\frac{kr}{\pi}\right)^{1/2} \sin \tfrac{1}{2}(\theta + \theta_0) \tag{31}$$

$$f(\sigma) = \frac{1+\mathrm{i}}{2} \int_{-\infty}^{\sigma} \mathrm{e}^{-\mathrm{i}\pi t^2/2}\, \mathrm{d}t \tag{32}$$

$$f(\sigma') = \frac{1+\mathrm{i}}{2} \int_{-\infty}^{\sigma'} \mathrm{e}^{-\mathrm{i}\pi t^2/2}\, \mathrm{d}t \tag{33}$$

A = arbitrary constant

t = dummy variable

Equation (32) can be rewritten as:

$$\begin{aligned} f(\sigma) &= \frac{1+\mathrm{i}}{2}\left[\int_{-\infty}^{0} \mathrm{e}^{-\mathrm{i}\pi t^2/2}\, \mathrm{d}t + \int_{0}^{\sigma} \mathrm{e}^{-\mathrm{i}\pi t^2/2}\, \mathrm{d}t\right] \\ &= \frac{1+\mathrm{i}}{2}\left[\frac{(1-\mathrm{i})}{2} + \int_{0}^{\sigma} \cos(\pi t^2/2)\, \mathrm{d}t - \mathrm{i}\int_{0}^{\sigma} \sin(\pi t^2/2)\, \mathrm{d}t\right] \\ &= \frac{1+\mathrm{i}}{2}\left[\frac{1-\mathrm{i}}{2} + M - \mathrm{i}N\right] \end{aligned} \tag{34}$$

where

$$M = \int_{0}^{\sigma} \cos(\pi t^2/2)\, \mathrm{d}t \tag{35}$$

$$N = \int_{0}^{\sigma} \sin(\pi t^2/2)\, \mathrm{d}t \tag{36}$$

M and N are the Fresnel integrals which are evaluated numerically by using asymptotic series (for $r \geq 8$) and Maclaurin series (for $r < 8$). The solutions of both series are widely available on computers. In this case the Algol 68-R library function 'FRESNEL' has been used.

In the computation of the diffraction waves, three regions have been considered (see Figure 1). Within each of these regions the wave effects are different. Region S is bounded by the breakwater and sheltered from the direct action of the incident wave. The waves reaching this region are only affected by diffraction. Region R is defined by the direction of the reflected wave passing through the breakwater tip, and breakwater itself. It consists of incident, reflected and diffracted waves. Region Q is located between regions R and S. It contains primarily the incident wave energy but is also affected by diffraction near the boundaries.

The wave height in any of the three regions can be calculated by the following formulae.

In region S:

$$F(r, \theta) = \underbrace{f(\sigma) \exp[-ikr \cos(\theta - \theta_0)] + f(\sigma') \exp[-ikr \cos(\theta + \theta_0)]}_{\text{diffracted wave}} \tag{37}$$

In region Q:

$$F(r, \theta) = \underbrace{\exp[-ikr \cos(\theta - \theta_0)]}_{\text{incident wave}}$$
$$\underbrace{-f(-\sigma) \exp[-ikr \cos(\theta - \theta_0)] + f(\sigma') \exp[-ikr \cos(\theta + \theta_0)]}_{\text{diffracted wave}} \tag{38}$$

In region R:

$$F(r, \theta) = \underbrace{\exp[-ikr \cos(\theta - \theta_0)]}_{\text{incident wave}} + \underbrace{\exp[-kr \cos(\theta + \theta_0)]}_{\text{reflected wave}}$$
$$\underbrace{-f(-\sigma) \exp[-ikr \cos(\theta - \theta_0)] + f(-\sigma') \exp[-ikr \cos(\theta + \theta_0)]}_{\text{diffracted wave}} \tag{39}$$

RESULTS

The aim was first to test the finite and infinite element numerical model on the classical diffraction problem. To see how well it reproduced the analytical solution. Then other problems, which have not, to date, been solved analytically, were analysed.

Diffraction by semi-infinite breakwater

One of the difficulties associated with numerical modelling of the diffraction problem is that there is a singularity in the velocity at the breakwater tip. That singularity is of the form

$$\nabla \phi \sim r^{-1/2}$$

It can however be modelled quite effectively using a technique which was originated in the field of elasticity by Henshell and Shaw.[16] Their method was to deliberately move the midside node of the 8 node isoparametric element to the quarter point, which induces a singularity in the element at the closest corner. This is because the Jacobian matrix is no longer invertible at that point. This singularity is of precisely the kind which is needed at the tip of the breakwater.

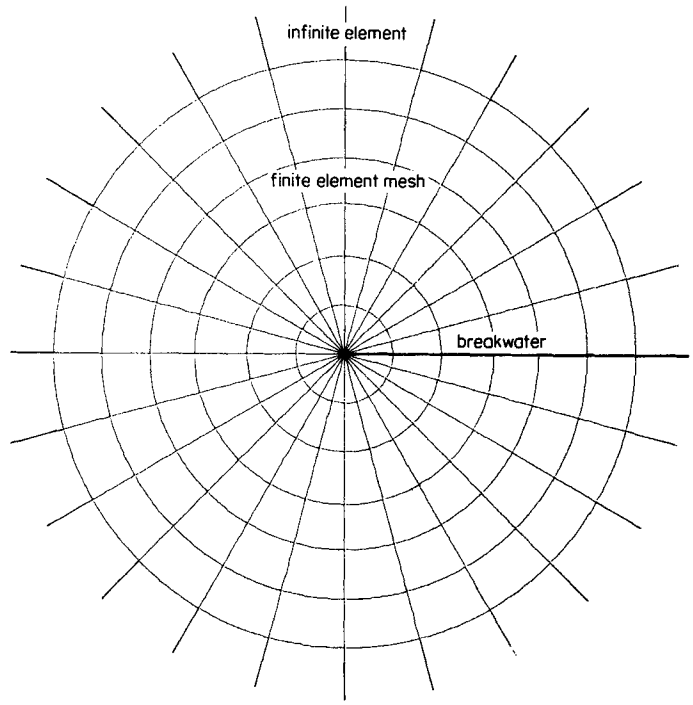

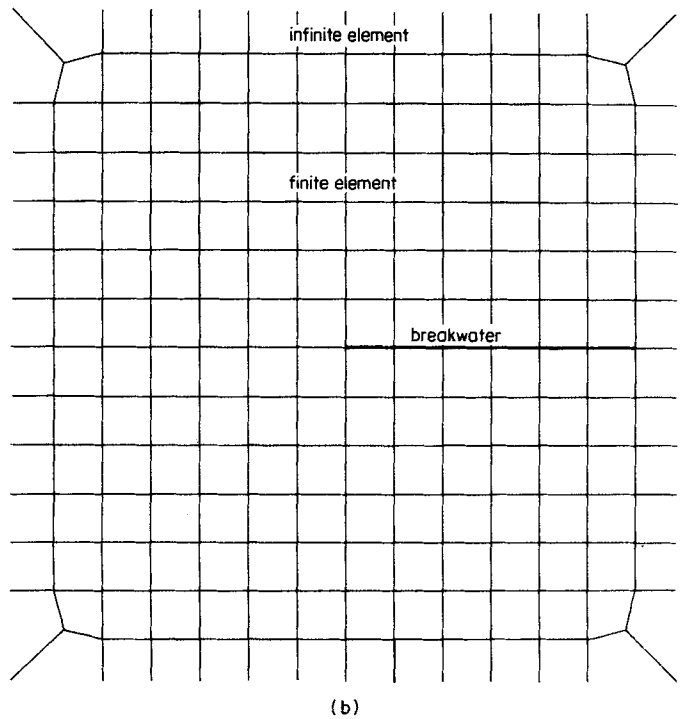

Figure 2. Element meshes (a) circular mesh; (b) square mesh

It should be noted that although this device enables the numerical technique to simulate the singularity found in the analytical solution, this singularity does not occur in real water waves. In the water waves the high velocity gradients at the tip of the breakwater produce viscous forces which retard the flow leading to separation and the formation of vortices. These may be observed in model tests. However the details of this flow are too complicated to be incorporated in this numerical model.

Two different meshes of elements were used for this problem, one based on a circle and the other on a square. The meshes are shown in Figures 2(a) and 2(b). Also shown is the detail of the positioning of the midside nodes in the finite elements at the tip of the breakwater, so as to induce an appropriate singularity there.

Figures 3 and 4 show the real and imaginary components of wave elevation along a line perpendicular to the breakwater and running through its tip, with and without the singularity induced at the tip. The wave data are as follows: $g = 9{\cdot}81$ m/s^2, $h = 15{\cdot}0$ m, $\omega = 0{\cdot}3142$ rad/s, $k = 0{\cdot}02590$ (1/m), $\lambda = 242{\cdot}610780$ m, $t = 20$ s and angle of incidence 90°. Figure 3 shows midside nodes in the first element put at midpoint and Figure 4 shows results when they are at quarter points. It is clear that displacing the midside nodes gives much better results in the vicinity of the breakwater tip. This shows that the Henshell technique for modelling the tip singularity is very effective. Both meshes were run for waves incident at 90° to the breakwater and also 45° and 135°. In Figures 5–7 contour plots of the absolute values of the

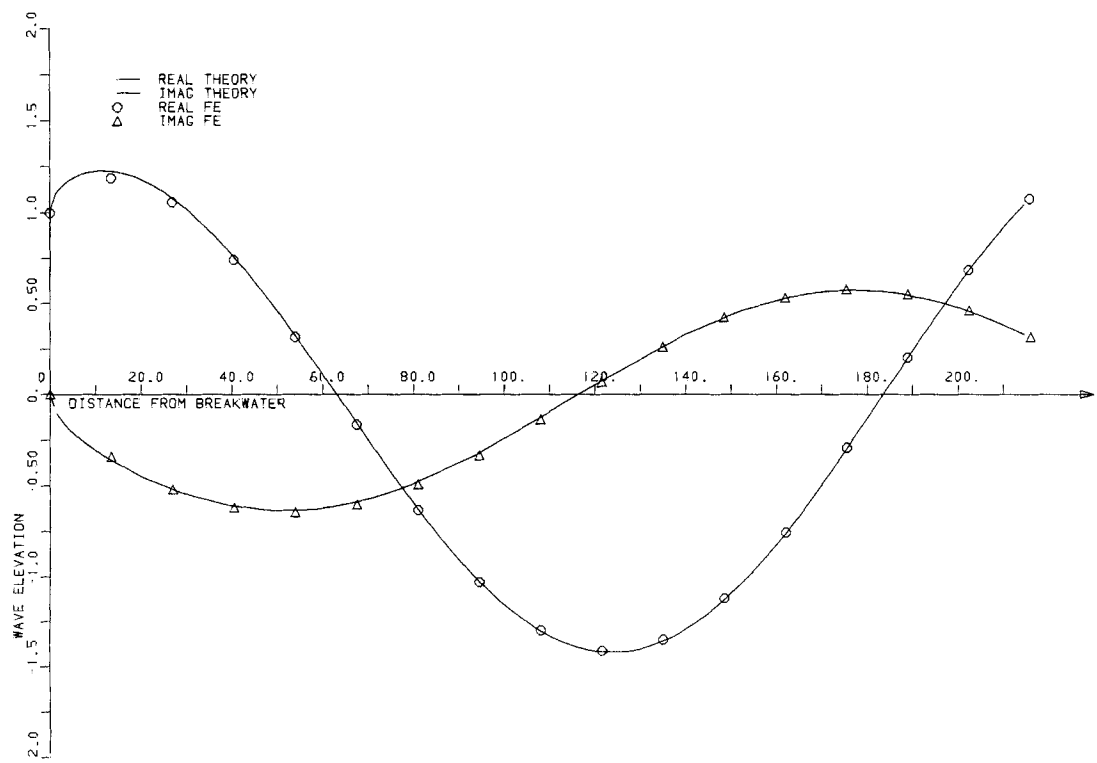

Figure 3. Semi-infinite breakwater—heights of diffracted waves. The wave heights on a line perpendicular to breakwater through tip: angle of incidence 90° to breakwater; wavelength = 242·610780 m; wave period = 20 s; mid-side nodes at mid-points

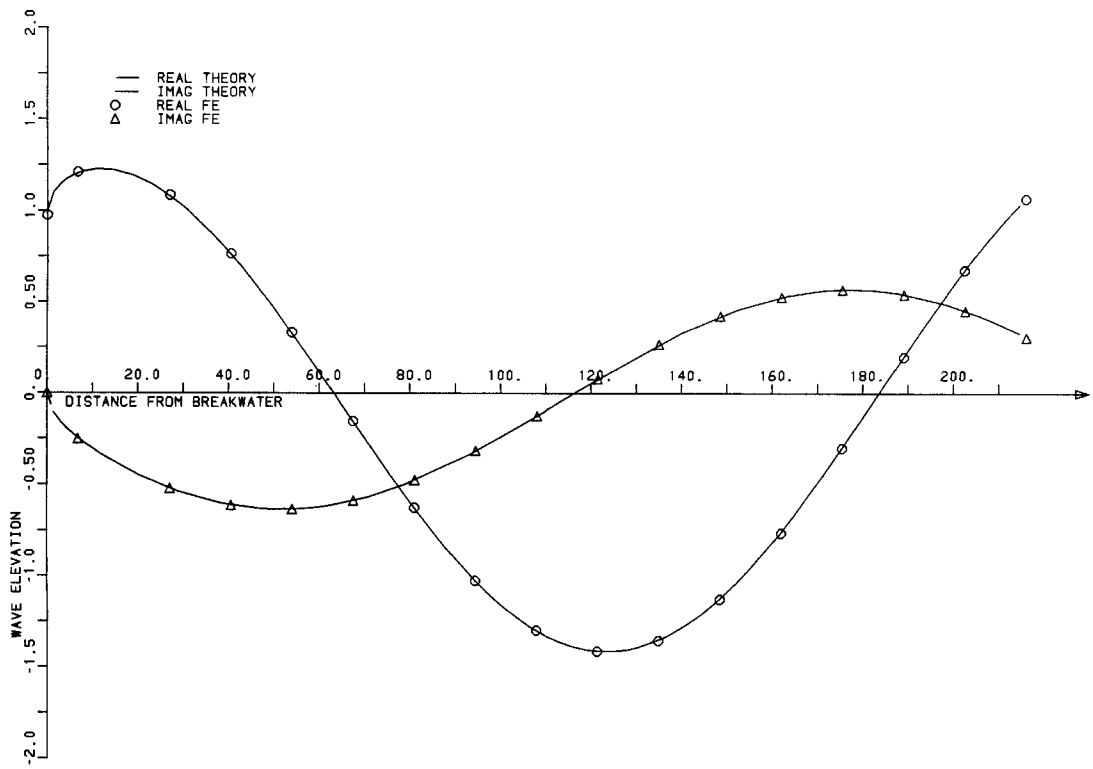

Figure 4. Semi-infinite breakwater—heights of diffracted waves. The wave heights on a line perpendicular to breakwater through tip: angle of incidence 90° to breakwater; wavelength = 242·610780 m; wave period = 20 s; mid-side nodes at quarter points

wave elevations are shown. In addition the analytical results were generated at the finite element nodes and the results were also processed by the finite element contour plotting program. Because of the large number of nodes this technique is accurate. It can be seen that the contour plots for finite element and analytical solutions are very similar. The two different shapes of mesh have no appreciable effect on the results. Figures 4, 8 and 9 show wave elevations plotted along lines perpendicular to the breakwater, and a comparison with the analytical values. Figures 10–12 show the effect of reducing the wavelength. The results become progressively less accurate as the wavelength is decreased. This is to be expected. As a general rule it is necesary to have about 4 elements per wavelength to obtain satisfactory resolution of the wave detail. If this restriction is satisfied good agreement is obtained with analytical solutions.

In the mesh shown in Figure 2(a) there are about 560 nodal unknowns. As they are complex this corresponds to approximately 1120 real unknowns. The main solution phase is carried out by the Irons frontal program, modified to deal with complex numbers. The total execution time was 335 s CPU on an ICL 2966, running under the DME operating system. The program and storage occupy 51 K 24 bit words of central memory. The program is organized so that it can be made to use more central memory if available, with less demand upon backing store.

In general halving the wave period will roughly halve the wavelength, and for the same physical extent of problem, a mesh with a subdivision twice as fine will be required. This

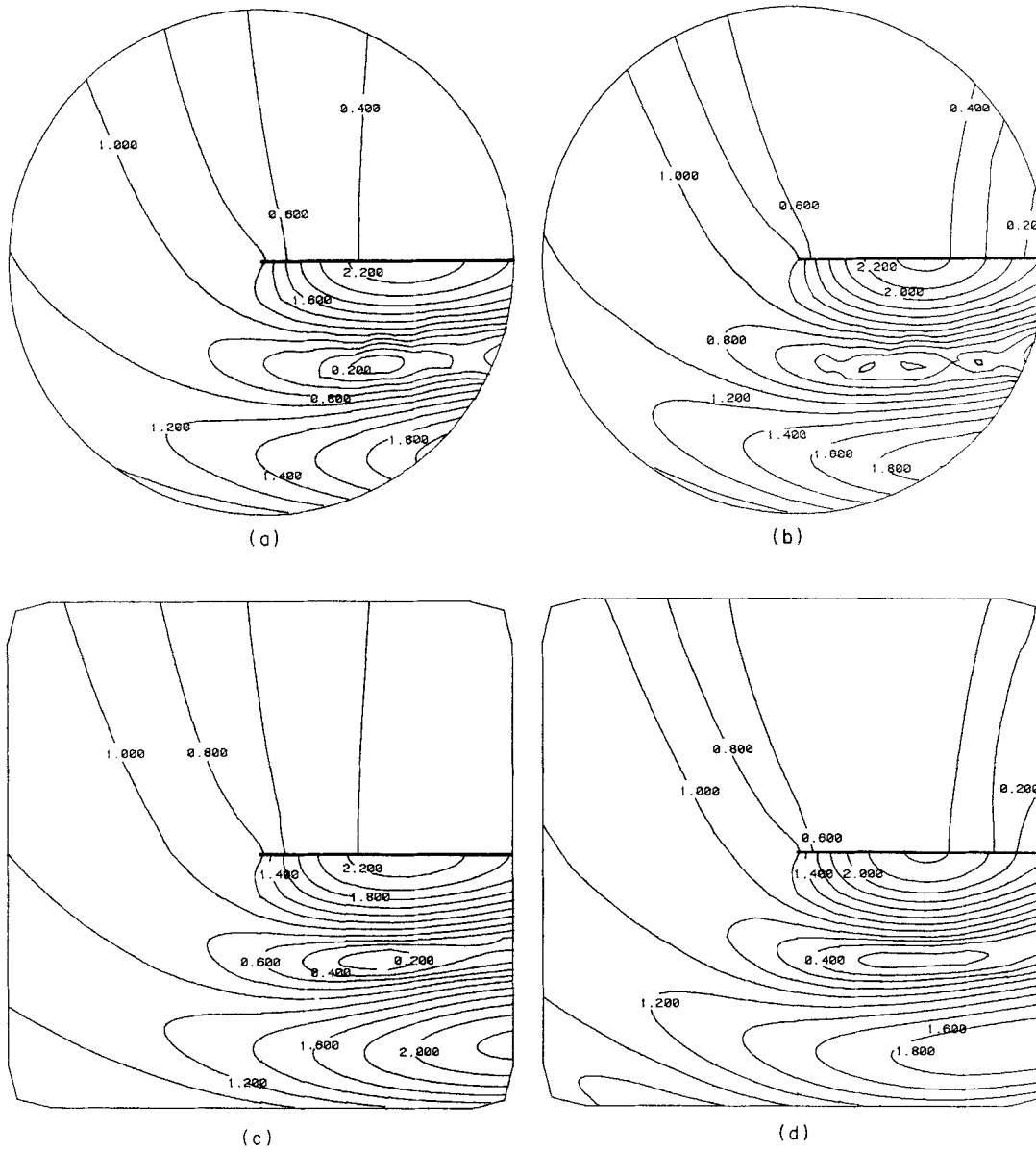

Figure 5. Contour of absolute values of wave height: wave amplitude = 1·0; wave period = 20 s; wavelength = 242·610780 m; accleration due to gravity = 9·81 m/(s)^2, angle of incidence = 90° (wave incident from bottom of page): (a) analytical solution evaluated at points in circular mesh; (b) numerical solution from finite and infinite elements in circular mesh; (c) analytical solution evaluated at points in square mesh; (d) numerical solution from finite and infinite elements in square mesh

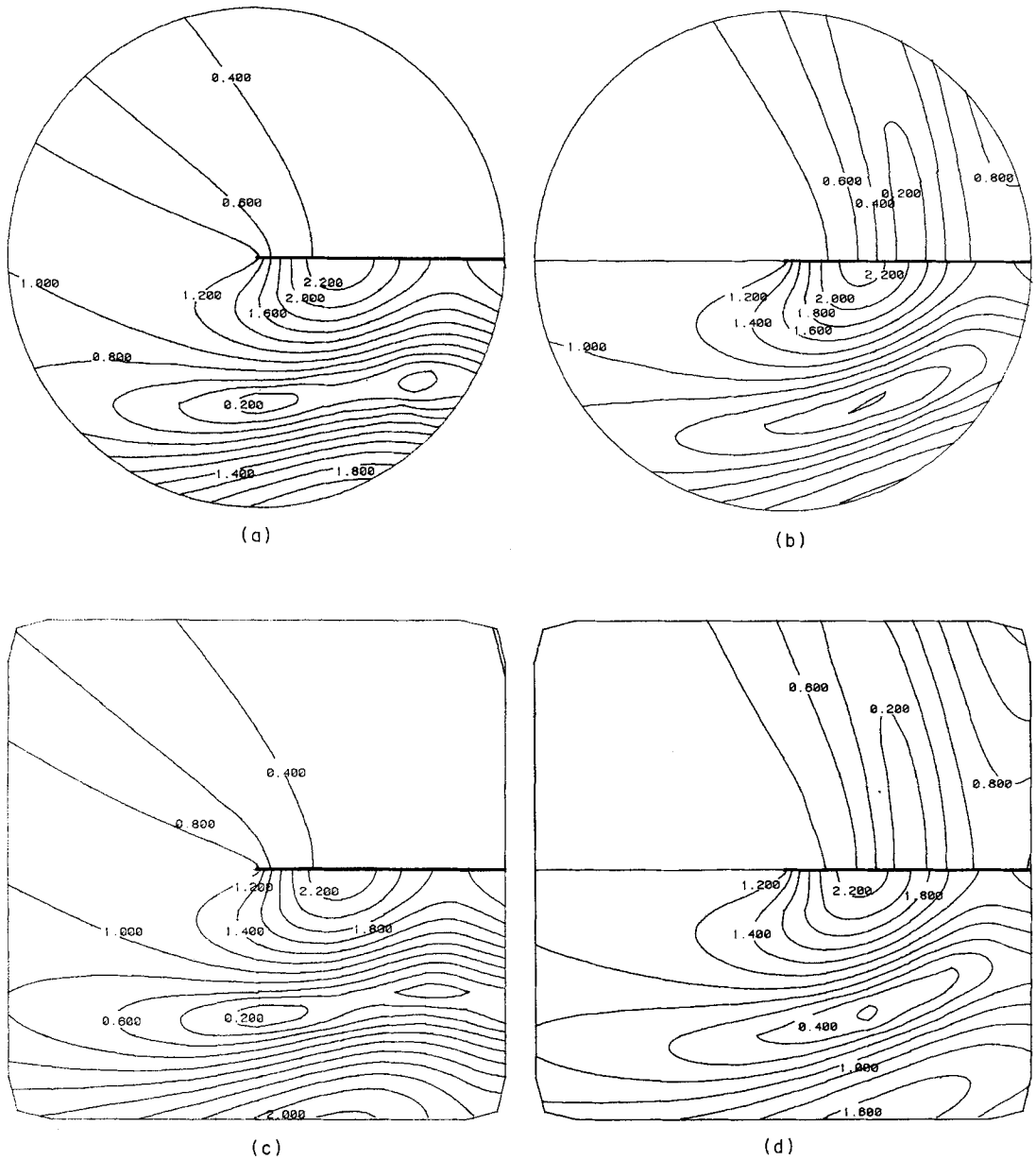

Figure 6. Contour of absolute values of wave height: wave amplitude = 1·0; wave period = 20 s; acceleration due to gravity = 9·81 m/(s)^2; angle of incidence = 45° (wave incident from bottom of page): (a) analytical solution evaluated at points in circular mesh; (b) numerical solution from finite and infinite elements in circular mesh; (c) analytical solution evaluated at points in square mesh; (d) numerical solution from finite and infinite elements in square mesh

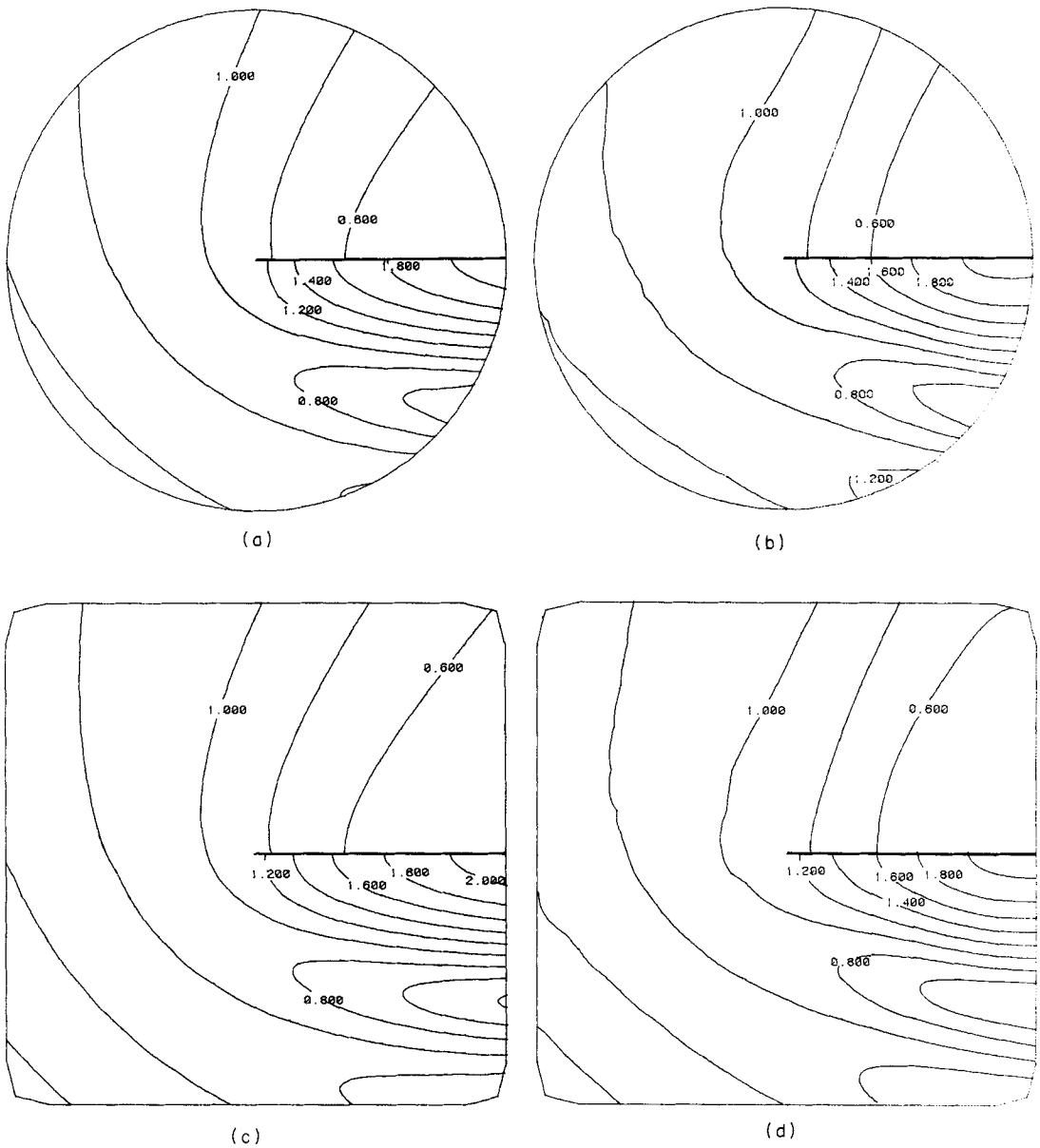

Figure 7. Contour of absolute values of wave height: wave amplitude = 1·0; wave period = 20 s; acceleration due to gravity = 9·81 m/(s)^2; angle of incidence = 135° (wave incident from bottom of page): (a) analytical solution evaluated at points in circular mesh; (b) numerical solution from finite and infinite elements in circular mesh; (c) analytical solution evaluated at points in square mesh; (d) numerical solution from finite and infinite elements in square mesh

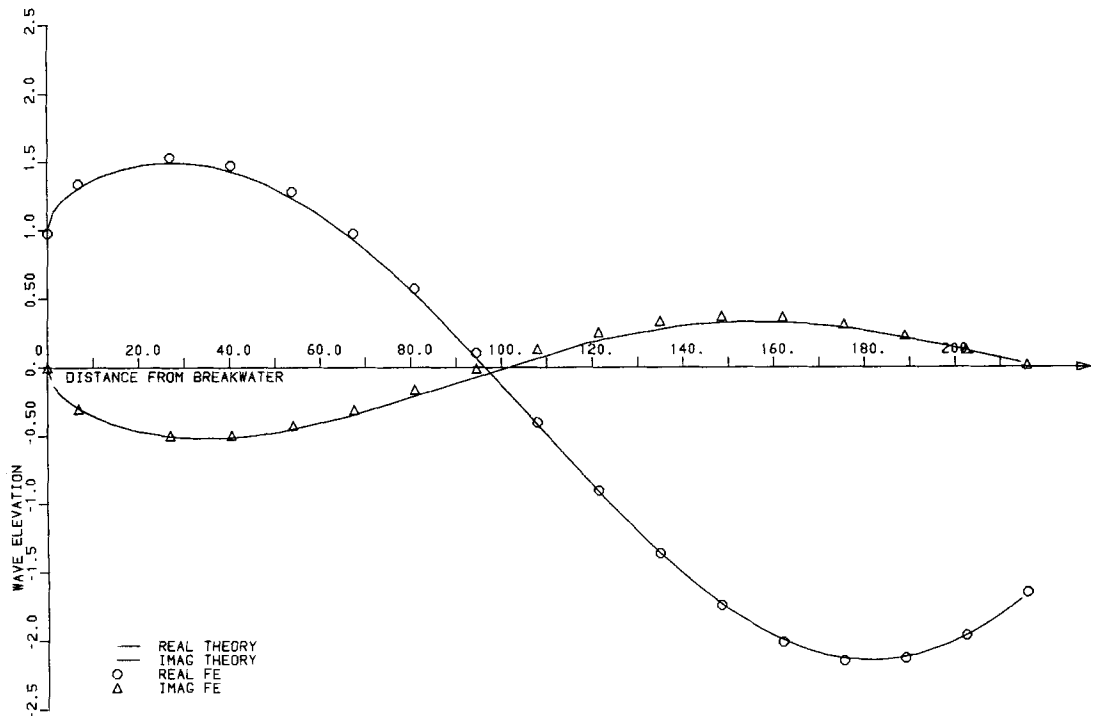

Figure 8. Semi-infinite breakwater—heights of diffracted waves. The wave heights on a line perpendicular to breakwater through tip: angle of incidence 45° to breakwater; wavelength = 242·610780 m; wave period = 20 s

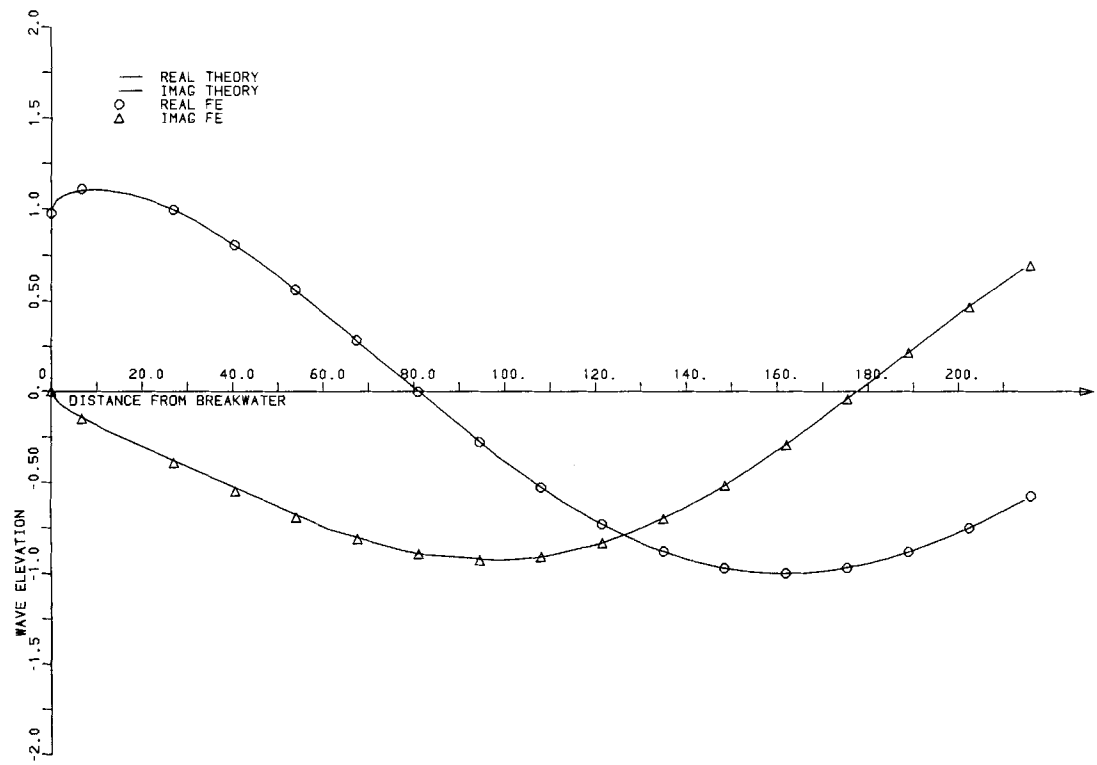

Figure 9. Semi-infinite breakwater—heights of diffracted waves. The wave heights on a line perpendicular to breakwater through tip: angle of incidence of 135° to breakwater; wavelength = 242·610780 m; wave period = 20 s

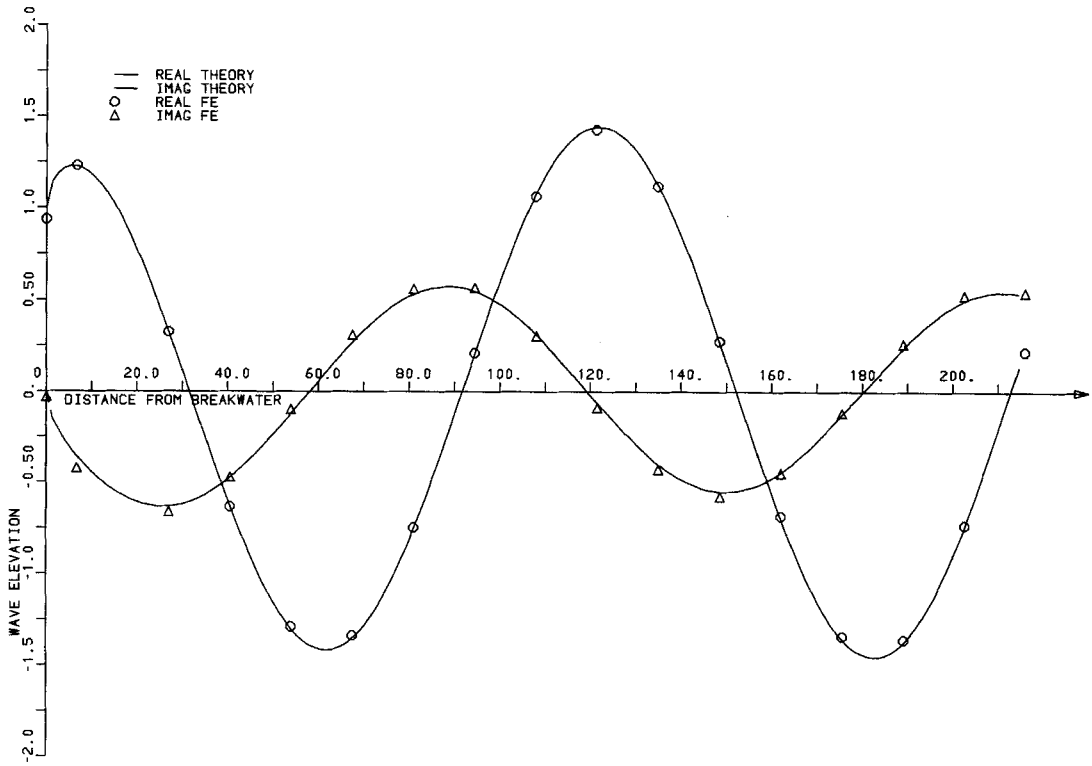

Figure 10. Semi-infinite breakwater—heights of diffracted waves. The wave heights on a line perpendicular to breakwater through tip: angle of incidence = 90° to breakwater; wavelength = 121·305390 m; wave period = 10 s

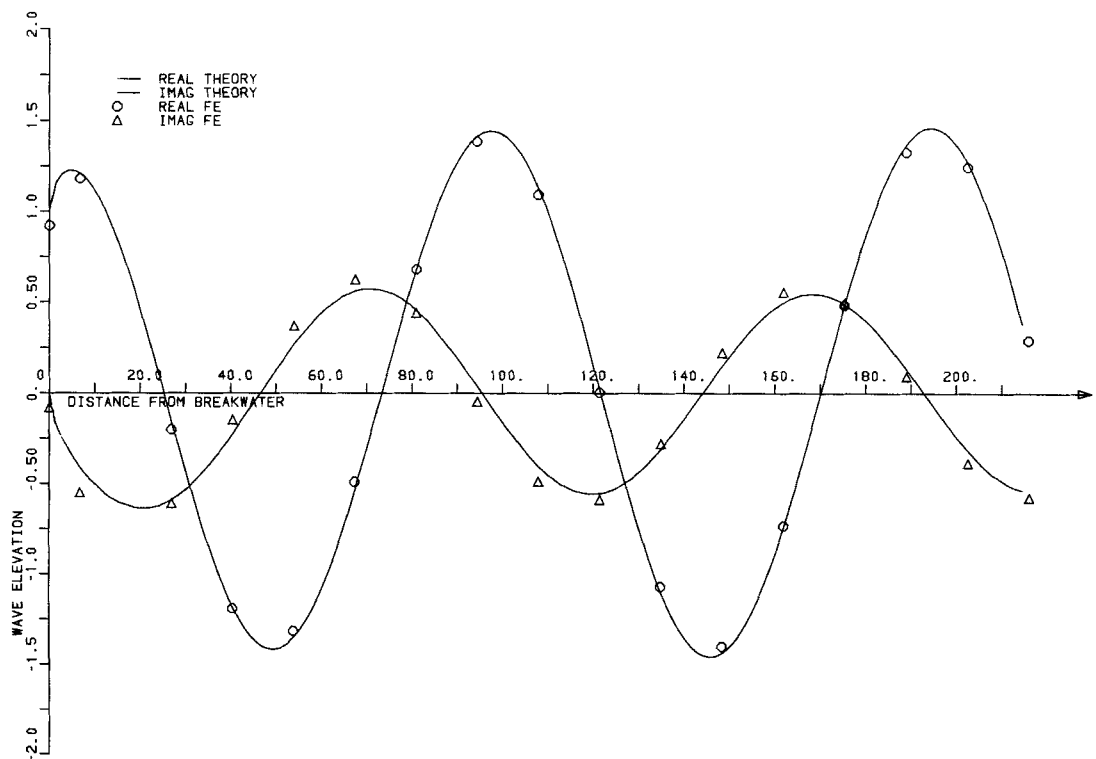

Figure 11. Semi-infinite breakwater—heights of diffracted waves. The wave heights on a line perpendicular to breakwater through tip: angle of incidence 90° to breakwater, wavelength = 97·0443120 m; wave period = 8 s

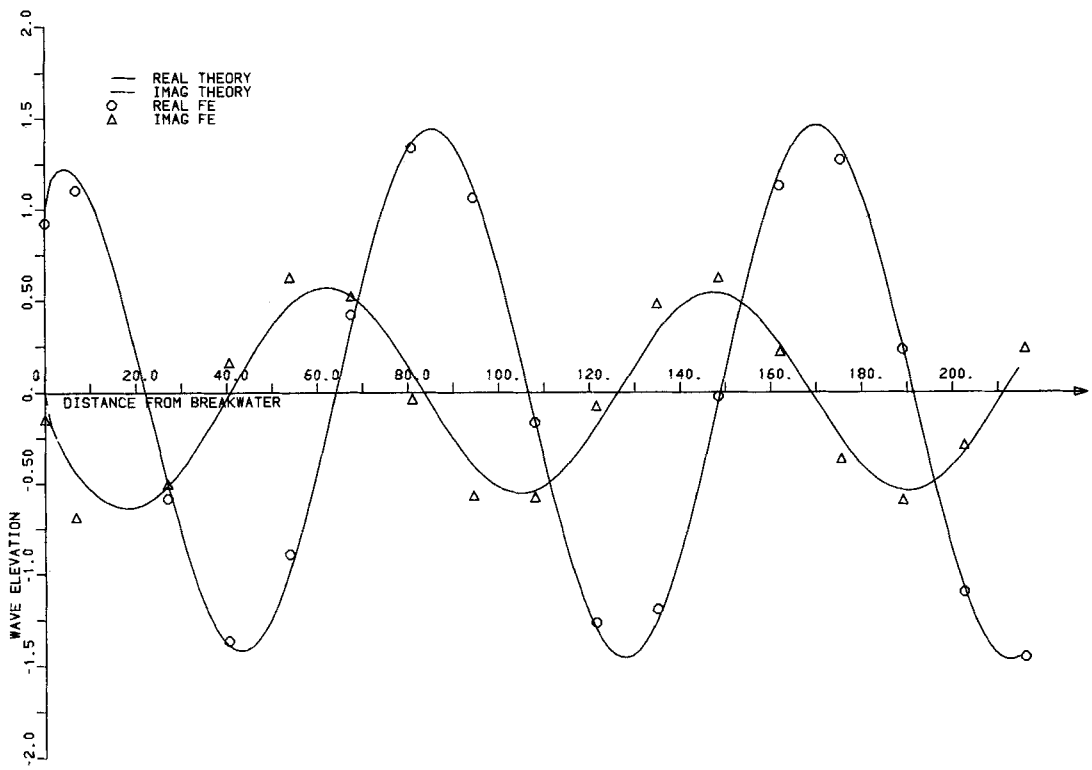

Figure 12. Semi-infinite breakwater—heights of diffracted waves. The wave heights on a line perpendicular to breakwater throught tip: angle of incidence = 90° to breakwater; wavelength = 84·913770 m; wave period = 7 s

increases the number of nodal unknowns by a factor of 4. So the storage will increase by a factor of 16 and the time by a factor of 64. (Since the number of storage locations is proportional to the square the number of unknowns and the number of operations is proportional to their cube.) The actual figures will not be quite as bad as this since it is only the dominant terms in the storage and operation requirements which are quadratic and cubic, respectively. However it is clear that, although in principle diffraction and refraction problems can be solved for any wavelength by this method, in practice the computing resources required increase very rapidly as the wavelength is reduced. It should perhaps be emphasized that in modern computers the terms of finite element analyses described in this paper are very small and quick. Wave problems with very short wavelengths are computable.

Diffraction and reflection by semi-infinite breakwater and parabolic shoal

To the semi-infinite breakwater originally considered is now added a parabolic shoal. The details of the geometry are shown in Figure 13. In Figure 14 the wave elevations are shown for a wave incident at an angle of 90° to the breakwater. A comparison of Figures 5 and 14 shows the changes to the wave pattern caused by the introduction of the shoal. The contours of absolute wave height are seen to be curved in towards the tip of the breakwater. Also the maximum amplitude, where the standing wave forms at the breakwater is 'sucked' in towards the tip and is increased in magnitude to 2·774 from 2·468 times the incident wave amplitude.

Figure 15 shows another example of a shoal and breakwater, with the results given in

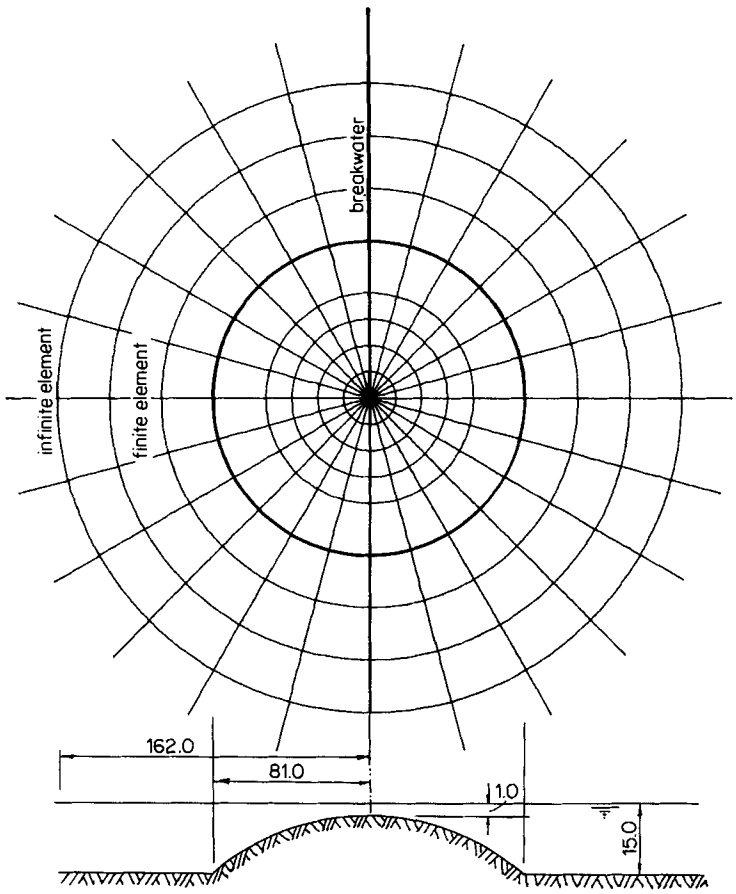

Figure 13. Geometry of parabolic shoal and element mesh. Finer mesh around the tip of breakwater

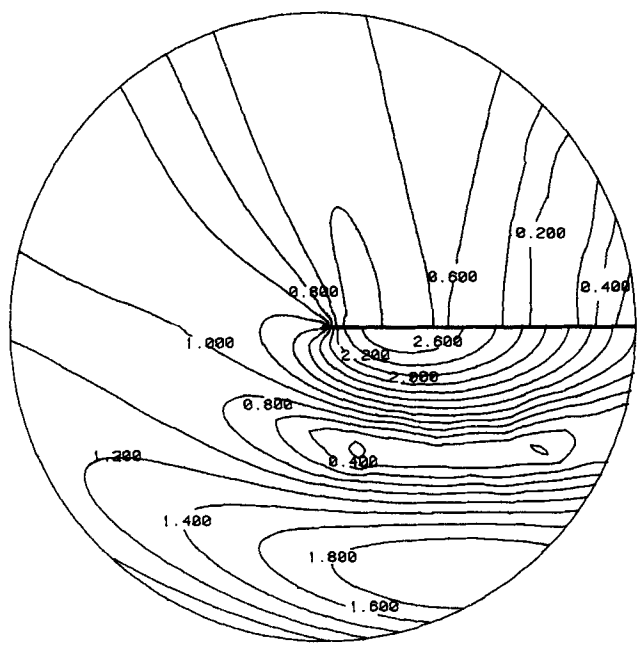

Figure 14. Wave elevations for a wave of wavelength incident at 90° to the breakwater. Finer mesh around the tip of breakwater

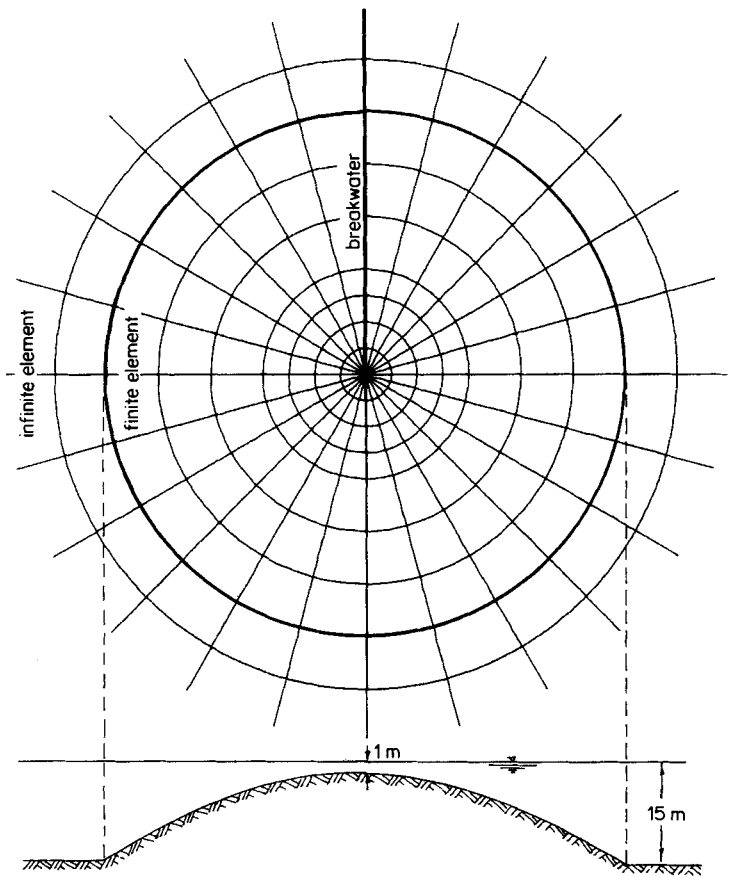

Figure 15. Geometry of shallower parabolic shoal and finer element mesh

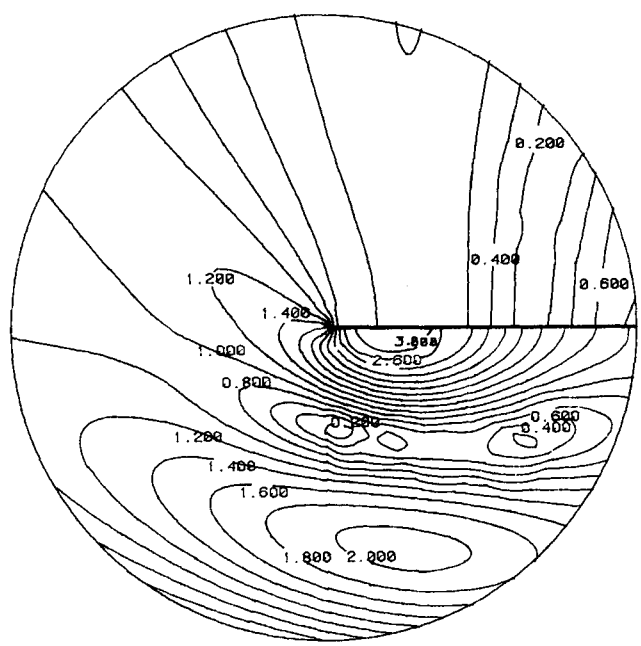

Figure 16. Wave elevations for a wave of wavelength incident at 90° to the breakwater

Figure 16. Again comparison may be made with Figure 5. In this case the shoal is more extensive and shallower and refraction is more marked. The peak value of wave elevation is now 3·212.

CONCLUSION

Finite and infinite elements used together are an effective and accurate way of modelling diffraction effects at breakwaters even if refraction is present. As discussed above the chief limitation of the technique is the fine mesh required when the incident wavelength is short. Even so with modern computing power, becoming increasingly cheaper, this is not a serious drawback.

REFERENCES

1. A. Sommerfeld, 'Theore mathematique de la diffraction', *Math. Ann.*, **47,** 317–374 (1896).
2. W. G. Penney and A. T. Price, 'Diffraction of sea waves by breakwaters', *Philosophical Transactions, Royal Society of London. Series A*, **244** (882), 231–253 (1952).
3. R. L. Wiegel, 'Diffraction of waves by semi-infinite breakwater', *Proc. ASCE, Paper No.* 3039, January (1962).
4. Shou-Shan Fan, J. E. Cumming and R. L. Wiegel, 'Computer solution of wave diffraction by semi-infinite breakwater', *Office of Research Services Technical Report HEL*-1-8, Berkeley, California, October 1967.
5. J. C. W. Berkhoff, 'Linear wave propagation problems and the finite element method', in (Eds.) R. H. Gallagher *et al.*, *Finite Elements in Fluids, Vol.* 1, Wiley, Chichester, 1975, p. 251.
6. J. C. W. Berkhoff, 'Computation of combined refraction-diffraction', *13th Int. Conf. Coastal Engng*, Vancouver, 1972.
7. D. Ian Austin and Peter Bettess, 'Longshore boundary conditions for numerical waves', *International Journal for Numerical Methods in Fluids*, **2,** 263–276 (1982).
8. O. C. Zienkiewicz and R. E. Newton, 'Coupled vibrations of a structure submerged in a compressible fluid', *Proc. Symp. Finite Element Techniques*, Institute fur Statik und Dynamik der Luft- und Baum- fahrtkonstruktionen, University of Stuttgart, Germany, 1969.
9. A. Sommerfeld, *Partial Differential Equations in Physics*, Academic Press, New York, 1949.
10. F. Rellich. 'Uber deas asymptotische Verhalten der Losungen von $\Delta u + \lambda u = 0$ in unendlichen Gebieten', *Jahresbericht der Deutschen Mathematiker Vereinigung*, **53,** 57–63 (1943).
11. R. Courant and D. Hilbert, *Methods of Mathematical Physics, Vol. 1*, Interscience, New York, 1966.
12. O. C. Zienkiewicz, *The Finite Element Method in Engineering Science*, McGraw-Hill, London, 1971.
13. A. Ralston, *A First Course in Numerical Analysis*, McGraw-Hill, New York, 1965.
14. P. Rabinowitz and G. Weiss, 'Tables of abscissas and weights for numerical evaluation of integrals of the form $\int_0^\infty e^{-x} x^n f(x)\,dx$', *Mathematical Tables and Other Aids to Computation*, **13,** 285–294 (1959).
15. P. Bettess and O. C. Zienkiewicz, 'Diffraction and refraction of surface waves using finite and infinite elements', *Int. J. Num. Meth. Eng.*, **11,** 1271–1290 (1977).
16. R. D. Henshell and K. G. Shaw, 'Crack tip finite elements are unnecessary', *Int. J. Num. Meth. Eng.* **9,** 495–507 (1975).